Biosensors and Bioelectronics 55 (2014) 113–119

Contents lists available at ScienceDirect

Biosensors and Bioelectronics

journal homepage: www.elsevier.com/locate/bios

An amperometric β-glucan biosensor based on the immobilization of bi-enzyme on Prussian blue–chitosan and gold nanoparticles–chitosan nanocomposite films

Beibei Wang, Xueping Ji *, Haiyan Zhao, Na Wang, Xianrui Li, Ruixing Ni, Yuheng Liu

Department of Medical Chemistry, Hebei Medical University, Shijiazhuang 050017, China

ARTICLE INFO

Article history:
Received 29 September 2013
Received in revised form
27 November 2013
Accepted 1 December 2013
Available online 10 December 2013

Keywords:
Biosensor
Prussian blue
Gold nanoparticles
β-glucanase
Chitosan
β-glucan

ABSTRACT

A novel β-glucan biosensor was fabricated by immobilizing β-glucanase (β-G) with glucose oxidase (GOD) on nano-Prussian blue–chitosan (PB–CS) and gold nanoparticles–chitosan (AuNPs–CS) composites. Both the PB–CS and AuNPs_CS film were directly electrodeposited on the surface of gold electrode. The morphology of the AuNPs–CS/PB–CS nanocomposites was characterized by scanning electron microscope (SEM). The electrochemical behavior of the resulting sensor was investigated using cyclic voltammetry (CV) and amperometry. It was found that PB–CS nanocomposite exhibited an excellent electrocatalytic reduction towards hydrogen peroxide at a low applied potential window. The synergistic effect of AuNPs–CS/PB–CS nanocomposites could remarkably improve the performances of the biosensor. Under optimal conditions, the biosensor showed a wide linear range of 6.25–93.75 μM, with a correlation coefficient of 0.9991. The sensitivity at an applied potential of 0.0 V was 100 nA μM^{-1} cm^{-2}, with a detection limit of 1.56 μM. The apparent Michaelis–Menten constant (K_m) was found to be 1.0 mM, showed a high affinity of the immobilizing β-G for β-glucan. The biosensor displayed a rapid response (within 10 s) toward β-glucan, with a good selectivity and stability.

1. Introduction

β-glucan, a natural polymer of D-glucose with (1→3), (1→4) and/or (1→6) glycosidic link-ages, exists in the cell walls of yeast, fungi and cereal plants. Numerous research have confirmed the health benefits of β-glucan, including lowering blood cholesterol and glycemia, antibacterial, immune-modulating (Gamel et al., 2013; Regand et al., 2011; Yuan et al., 2009). In recent years, β-glucan has attracted increasing research interest due to its extensive application in food and medicine fields. Therefore, it is very important to detect β-glucan concentration for clinical diagnosis, drug and food control.

Various methods are available for the determination of β-glucan, including viscometric, colorimetric method, enzymatic method, and immune recognition method (G-test, dectin-1) (Wood et al., 1989; Clavaud et al., 2012; Pastuszka et al., 2012; Koichiro et al., 2012). These methods are often time-consuming, and require well trained personnel to perform. At present, electrochemical biosensor has been proven to be an accurate and versatile method for analytical applications, due to some advantages of high selectivity and sensitivity, relatively low cost, the potential for miniaturization, and the possibility of in situ analysis (Sanchez-Paniagua Lopez et al., 2009; Park et al., 2012).

However, to our knowledge, there are very few literatures available on β-glucan biosensor. For example, Bagal-Kestwal et al. (2010) have developed β-glucan bi-enzyme biosensor and tri-enzyme biosensor based on the immobilization of enzymes with gold nanoparticles (AuNPs) in agarose–cornflour–gelatin matrix. Both the bi-enzyme biosensor and tri-enzyme biosensor had low detection limit and high sensitivity for β-glucan. However, the bi-enzyme biosensor, with a relatively high applied potential of 200 mV vs. standard calomel electrode (SCE), caused easily interference from co-existents in real samples. The tri-enzyme biosensor had several drawbacks such as high cost, relatively low reusability and poor operational stability. Therefore, it is important for searching some methods to improve the electrochemical performance of the biosensors.

Prussian blue (PB) plays an important role in the field of biosensors due to its analogy with the peroxidase enzymes, which exhibits good electrocatalytic activity towards hydrogen peroxide reduction at low overpotential (Bai et al., 2013; Che et al., 2010; Karyakin et al., 2000). As far as we know, PB-based nanocomposites are usually used for the immobilization of glucose oxidase (GOD) to fabricate glucose biosensor (Ji et al., 2010; Wang et al.,2012; Che et al., 2010), but has not been used for the construction of glucan sensor so far.

* Corresponding author. Tel.: +86 311 86265593.
E-mail addresses: xuepingji@126.com, xpji03@yahoo.com.cn (X. Ji).

0956-5663/$ - see front matter © 2013 Elsevier B.V. All rights reserved.
http://dx.doi.org/10.1016/j.bios.2013.12.004

Additionally, the signal amplification and the stable immobilization of the enzymes are of considerable importance for the construction of biosensors. In recent decades, metal nanoparticles, especially for AuNPs, have been successfully used in the fabrication interface of biosensors to enhance their electronic, chemical, and electrochemical properties due to its unique chemical and physical properties (Batra and Pundir, 2013; Hou et al., 2012; Koh et al., 2011). The AuNPs can facilitate electron transfer and produce signal amplification in electrochemical detection as a sensor platform. However, the pure nanoparticles have several drawbacks of lack of stability and uniform particle distribution. To overcome the problems, the incorporation of nanoparticles with polymers (Gu et al., 2009, Yang et al., 2012; Zhong et al., 2012; Bai et al., 2013) has attracted increasing interest in improving the stability and biocompatibility to enhance the capability of immobilization. Among them, the biopolymer chitosan (CS) has been proven particularly useful in the development of biosensors due to its low cost, ready film forming ability, nontoxicity, chemical and electrochemical stability (Ji et al., 2010). Several reports have demonstrated that nano-composite films display a three-dimensional (3-D) superstructure with higher electrocatalytic activity, stability and uniform particle distribution (Zhong et al., 2012; Du et al., 2007; Mbhele et al., 2003; Zhang et al.,2012).

In the present work, we developed a β-glucan biosensor based on the immobilization of bi-enzyme on PB–CS/AuNPs–CS nano-composite films. The PB–CS and AuNPs–CS were directly electrodeposited onto the gold electrode successively, instead of the traditional chemical method. Subsequently, the β-glucanase (β-G) was co-immobilized with GOD on the nano-composite films by using chitosan as a sealing agent coating on the outer layer to prevent the leakage of enzymes. The use of PB, instead of peroxidase, is beneficial to reduce cost and improve the operation stability. The introduction of chitosan not only can offer a suitable microenvironment to maintain the biological activity of the enzymes, but also can form a compact network structure to effectively prevent the leakage of the enzymes due to its excellent film forming ability, biocompatibility, good adhesion (Ji et al., 2010). The proposed biosensor was successfully applied to the detection of β-glucan in real samples.

2. Experimental

2.1. Materials and chemicals

Chitosan (CS, MW 1.5×10^5, 75–85% deacetylation) was obtained from Yuhuan Chemical Factory (Zhejiang, China). β-glucanase (β-G, from *Aspergillus niger*, 1.36 unit mg^{-1}) and glucose oxidase (GOD, from *A. niger*, 10,000 unit mg^{-1}), obtained from Sigma, were used without further purification. β-glucan was purchased from Sinopharm Chemical Reagent Co. Ltd. (China). Ascorbic acid (AA), acetaminophen (AP) and uric acid (UA) were purchased from Tianjin Kaitong Chemical Reagent Co. Ltd. (China). Glutaraldehyde solution (50%) was obtained from Tianjin Kemiou Chemicals Factory (China). Potassium ferricyanide was the product of Shanghai Chemical Reagent Factory (Shanghai, China). Hydrogen peroxide (H_2O_2, 30% w/v) and ferric chloride were purchased from Tianjin Yongda Chemical Reagent Development Center (China), and used as received. The exact concentration of H_2O_2 was obtained by titration with a standard potassium permanganate solution. All other chemicals were of analytical reagent grade, and used as received.

Phosphate buffer solutions (PBS, 0.10 M, pH 7.0) were prepared from disodium hydrogen phosphate and potassium dihydrogen phosphate (Tianjin Chemical Reagent Factory, Tianjin, China), with the pH adjusted with potassium hydroxide or phosphoric acid.

A 1 wt% chitosan solution was prepared by dissolving 1.0 g of chitosan flakes into 100 mL of 1.0% acetic acid and stirred for 10 h at room temperature until complete dissolution. The chitosan solution was filtered by a 0.45 μm syringe filter, and then stored in a refrigerator when not in use.

A 10% β-glucan stock solution was prepared in 0.10 M PBS (pH 7.0).

2.2. Apparatus

All electrochemical experiments were performed using a computer-controlled CHI 750C electrochemical workstation (CH Instruments, Chenhua Co., Shanghai, China) at ambient temperature (23 ± 2 °C). A conventional three-electrode system was used. The working electrode was a modified Au electrode, and the reference electrode was a Ag/AgCl (3 M KCl). The counter electrode was a platinum wire.

In amperometric experiments, the current-time data were recorded by applying a potential of 0.0 V on a stirred cell after a constant residual current had been established and a β-glucan solution was successively added into the buffer solution. The response current was marked with the change value of the steady state current and the background current. Cyclic voltammetry (CV) measurements were carried out in quiescent solutions with the scan rate of 20 mV s^{-1}. Surface morphology of the modified electrodes was characterized by a scanning electron microscope (SEM, S-4800, Japan).

2.3. Preparation of biosensor

The gold disk electrodes (2 mm Φ) were carefully polished first with a 1200 grit Carbimet disk, and then followed by 1.0, 0.3 and 0.05 mm alumina slurry on microcloth pads. After removing the trace alumina from the surface by rinsing with water at each step, the electrodes were ultrasonicated for 10 min in a fresh Piranha solution (H_2SO_4:H_2O_2=3:1 (v/v)). *Warning*: *Piranha solution reacts violently with organic solvents*. The electrodes were then ultrasonicated in water, acetone, and water again for 5 min, respectively. After being rinsed with water and dried, the electrochemical deposition of PB–CS nano-composite film on the surface of electrode was carried out by potential cycling in an unstirred fresh 0.10 M KCl+0.01 M HCl+0.5 mM $K_3[Fe(CN)_6]$+0.5 mM $FeCl_3$+0.01% CS solution (pH 2.0) in the potential range of −0.1 to +0.45 V at a scan rate of 20 mV s^{-1}. The amount of the PB–CS nano-composite film electrodeposited on Au electrode was controlled by scanning cycle, which took 10 cycles to obtain the optimal amount of the PB–CS nano-composite film. The PB–CS/Au electrode was then rinsed carefully with water and dried. After that, AuNPs–CS nano-composite film was electrodeposited on the PB–CS/Au by chronoamperometry in 0.1% $HAuCl_4$+0.025% CS solution (pH 5.0) at −0.2 V for 180 s. The AuNPs–CS/PB–CS/Au electrode was rinsed with water and dried at room temperature. After that, an aliquot of 5 μL of bi-enzyme mixed solution (β-G: 0.068 units; GOD: 125 units) was dropped onto the surface of the AuNPs–CS/PB–CS/Au electrode and nearly dried in a refrigerator at 4 °C. Then an aliquot 5 μL of 1% CS solution was dropped onto the surface of the β-G-GOD/AuNPs–CS/PB–CS/Au electrode and nearly dried. Finally, the enzyme electrode without rinse was dip-coated by 5 μL of 0.25% glutaraldehyde cross-linking ca. 30 min. The resulting CS/β-G-GOD/AuNPs–CS/PB–CS/Au electrode was thoroughly washed with water, and then stored in 0.10 M PBS (pH 7.0) at 4 °C for future use.

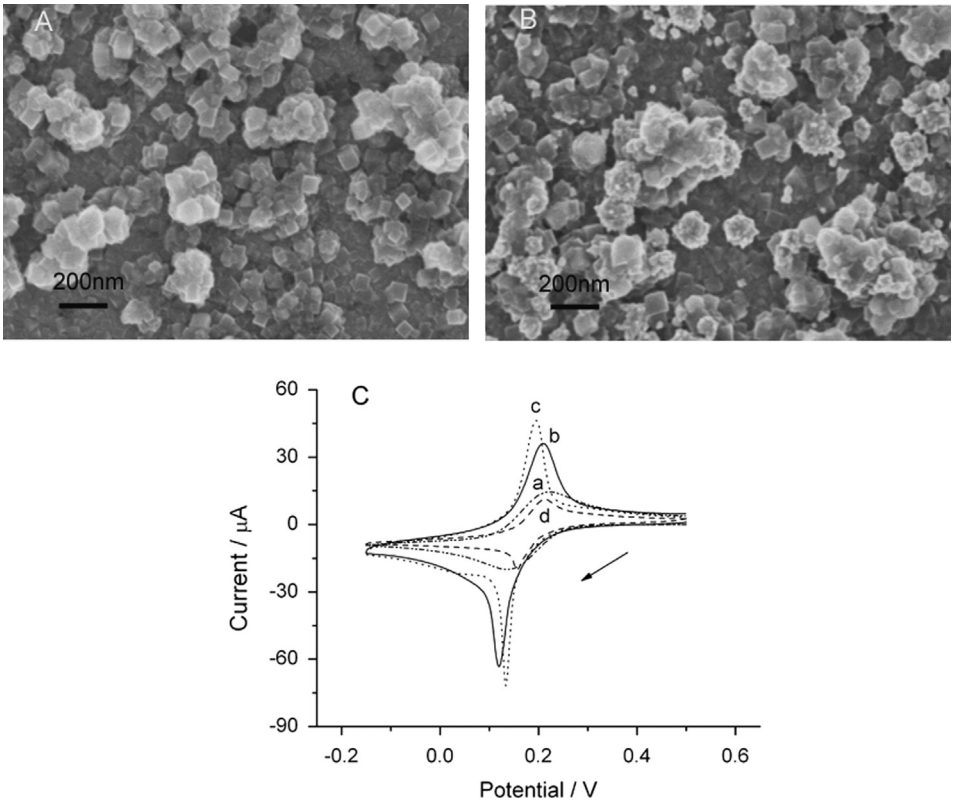

Fig. 1. SEM images of PB–CS nano-composite film (A) and AuNPs–CS/PB–CS nano-composite film (B). (C) CVs obtained from different modified electrodes in 5 mM $[Fe(CN)_6]^{3-}$/$[Fe(CN)_6]^{4-}$ containing 0.1 M PBS at a scan rate of 20 mV s^{-1}. (a) Bare Au, (b) PB–CS/Au, (c) AuNPs–CS/PB–CS/Au, and (d) CS/β-G-GOD/AuNPs–CS/PB–CS/Au electrode.

3. Results and discussion

3.1. Characterization of nano-composite films

SEM was employed to characterize the morphology of the electrodeposited PB–CS and AuNPs–CS/PB–CS nano-composite films on Au electrode. Fig. 1(A) shows the SEM image of the PB–CS nano-composite film. It can be observed that PB nanocubes, with an average size of 50 nm, were homogeneously spread out on the surface of the electrode. Fig. 1(B) shows the SEM image of AuNPs–CS/PB–CS nano-composite film. It can be found that AuNPs embedded in chitosan film, which wrapped PB nanocubes, forming stable and uniform nanocomposite films. It can be explained as follows. Chitosan has a pK_a of 6.5 (Sorlier et al., 2001). It is positively charged at pH 5.0 due to some of its amino groups protonated. The positively charged chitosan polyelectrolyte could strongly absorb anions such as $AuCl_4^{-1}$, $[Fe(CN)_6]^{3-}$ via electrostatic interactions (Zhang et al., 2008), which could favor the formation of the AuNPs–CS/PB–CS nanocomposites. The interaction between chitosan and nanoparticles could enhance the stability of the nanocomposites to some extent (Song et al., 2011; Wang et al., 2009; Zhang et al., 2012).

3.2. Electrochemical behavior of the biosensor

The assembly process of the modified electrode was monitored by CV using $[Fe(CN)_6]^{3-}$/$[Fe(CN)_6]^{4-}$ as a redox probe. The cyclic voltammograms (CVs) of different modified electrodes in 5 mM $[Fe(CN)_6]^{3-}$/$[Fe(CN)_6]^{4-}$ solution at a scan rate of 20 mV s^{-1} are shown in Fig. 1(C). It can be seen that a pair of reversible redox peaks, characteristic of a diffusion-limited redox process, was observed at the bare Au electrode (Fig. 1(C), curve a). After the electrodeposition of PB–CS on the surface of the electrode, the redox peak currents (Fig. 1(C), curve b) obviously increased, and peak potential separation (ΔE_p, the potential difference between the oxidation and reduction peak potentials) changed narrow. The increase of peak currents resulted from the conversion between Prussian white (PW) and PB (Zeng et al., 2008). With the assembly of AuNPs–CS nano-composite film (Fig. 1(C), curve c), the redox peak currents increased further. It may be attributed to the excellent conductivity of the AuNPs which can act as an electron conducting tunnel or electrical wire and promote the transmission of electrons between the redox probe and the underlying electrode (Ou et al., 2007; Zhao et al., 2006). On the assembly of CS/β-G-GOD composite film on the AuNPs–CS/PB–CS layer, the peak currents decreased (Fig. 1(C), curve d). This may be attributed to the non-conductivity of enzymes film, which hinders the access of the electrons to the electrode, compared with the AuNPs–CS/PB–CS modified electrode (Ji et al., 2010; Yang et al., 2006). These results above implied that PB–CS, AuNPs–CS, β-G-GOD/CS were successfully assembled onto the Au electrode.

3.3. Optimization of PB–CS/Au preparation and its electrocatalytic reduction towards H_2O_2

The characteristics of the PB–CS nano-composite film are influenced by several factors, including $K_3[Fe(CN)_6]$, $FeCl_3$ and CS concentration, deposition solution pH, and scanning time (scanning cycle).

The effect of $K_3[Fe(CN)_6]$, $FeCl_3$ and CS concentration on the properties of the deposited film was investigated in 0.1 M PBS (pH 7.0). According to previous report (Liu et al., 2002), the stoichiometric ratio of Fe^{3+} to $[Fe(CN)_6]^{3-}$ at 1:1 during pure PB formation, no Fe^{3+} were found in the resultant PB crystal. In this study, it was found that the concentration of $K_3[Fe(CN)_6]$ or $FeCl_3$ being more than 0.5 mM would result in precipitation from

solution after adding the chitosan in deposition solution. However, when the concentration of $K_3[Fe(CN)_6]$ or $FeCl_3$ was less than 0.5 mM, the rate of PB formation became slow. So we chose 0.5 mM as the optimum concentration of both $K_3[Fe(CN)_6]$ and $FeCl_3$ in further experiments. Recent studies have shown that chitosan could not only improve the stability of PB in neutral and alkalescent solution, but also prevent the PB nanoparticles from aggregating (Zhang et al., 2008; Chen et al., 2008). In order to investigate the effect of the chitosan concentration, the PB–CS film modified-electrode was prepared with 0.5 mM $K_3[Fe(CN)_6]$+ 0.5 mM $FeCl_3$ containing 0.10 M KCl and 0.01 M HCl with different concentrations of chitosan. Fig. S1 shows the CVs of the different modified electrodes in 0.1 M PBS. It was observed that on the addition of chitosan in deposition solution, the peak currents increased (Fig. S1, curve b), compared with chitosan-free deposition solution (Fig. S1, curve a), and along with the increase of the concentration of chitosan, the peak currents increased further (Fig. S1, curve c). However, when the concentration of chitosan was more than 0.01%, the deposition solution became turbid. So 0.01% was selected as the optimal concentrations of CS in deposition solution. The results demonstrated that the introduction of chitosan had a great impact on the structure and properties of the film. It has been reported that the surfaces of the CS-containing PB nanocomposites became rough and obscure (Zhong et al., 2012). The proposed mechanism for the formation of PB–CS is attributed to the fact that the chitosan, rich in amino, has chelating properties for metal cations (Zhang et al., 2008).

The proposed mechanism for the formation of 3-D PB–CS is attributed to the fact that the chitosan, rich in amino, has chelating properties for metal cations (Zhang et al., 2008).

The effect of the pH value on the properties of the PB–CS film was then investigated in the pH range from 2.0 to 4.0. As shown in Fig. S2, the response current increased with the decrease of the pH from 4.0 to 2.0. When the pH is less than 2.0, the deposition solution would be turbid. Thus, the deposition solution of pH 2.0 was selected for the electrodeposition of PB–CS film.

Finally, the effect of scanning time on the properties of the PB–CS film was investigated in 0.1 M PBS containing 4 mM H_2O_2. Fig. 2 shows the CV behavior of PB–CS film-modified Au in the presence or absence of H_2O_2. The modified electrode was prepared by depositing for 5 cycles under the conditions above. It was found that on the addition of 4 mM H_2O_2 into the 0.1 M PBS, an obvious increase of reductive peak current could be observed (Fig. 2, curve b), compared with that in the absence of H_2O_2 (Fig. 2, curve a), exhibiting the effective electrocatalytic reduction of the PB–CS towards H_2O_2. The current response of the PB–CS/Au electrode to H_2O_2 was dependent on the deposition cycle of the PB–CS film. Fig.2 (Inset) shows the dependence of the response current of the PB–CS/Au electrode to 4 mM H_2O_2 on the deposition cycle of the PB–CS film. It can be found that the reductive peak current decreased with the increase of scanning cycle. However, when scanning cycle were less than 10 cycles the PB–CS film was easily detached from the electrode in the air. Considering the response current and the stability of PB–CS film, we choose scanning cycle to be 10 cycles.

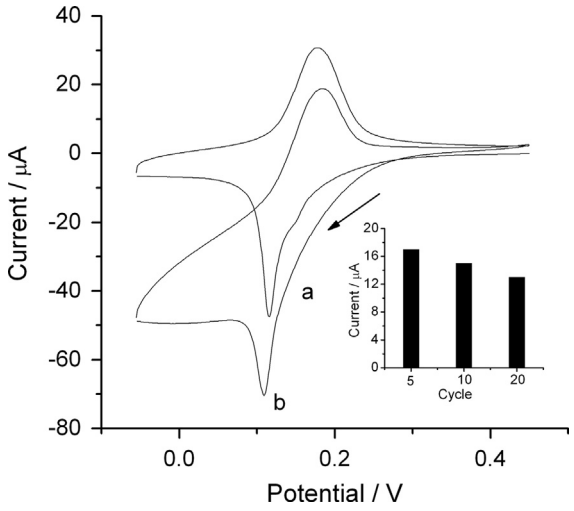

Fig. 2. CVs of the PB–CS/Au electrode in 0.1 M PBS containing 0.0 (a) and 4.0 mM H_2O_2 (b). Scan rate, 20 mV s^{-1}. Inset, dependence of the response current of the PB–CS/Au electrode to 4 mM H_2O_2 in 0.1 M PBS on the deposition cycle of the PB–CS film.

3.4. Optimization of AuNPs–CS film electrodeposition and enzyme loading

As has been reported, the characteristics of the AuNPs–CS nano-composite film are dependent on the concentration of $HAuCl_4$ and CS, deposition time, and applied voltage (Du et al., 2007). The effect of these deposition conditions on the response of the electrode was studied by CV.

The effect of $HAuCl_4$ and CS concentration on the properties of the AuNPs–CS deposited film are investigated in 0.1 M PBS (pH 7.0), as shown in Fig. 3(A) and (B). It was found that the maximum peak currents can be observed with 0.1% $HAuCl_4$ and 0.025% CS solution (pH 5.0) at an applied voltage of −0.2 V and a deposition time of 240 s. Fig. 3(C) is the CV response of AuNPs–CS nano-composite film deposited in 0.1% $HAuCl_4$+0.025% CS (pH 5.0) at an applied voltage of −0.2 V with different deposition times of 120 s, 180 s, and 240 s. It can be seen that the peak current reached the maximum when the deposition time was 180 s. Fig. 3 (D) shows the CVs of the different deposition voltages from −0.4 V to 0.0 V in 0.1% $HAuCl_4$+0.025% CS solution (pH 5.0) with the deposition time of 180 s. Similarly, from the Fig. 3(D), the maximum peak current was observed at −0.2 V.

Thus, we finally choose 0.1% $HAuCl_4$ and 0.025% CS solution (pH 5.0), the applied voltage of −0.2 V and the deposition time of 180 s as the AuNPs–CS electrodeposited conditions.

The amount of enzyme immobilized on electrode surface is an important factor affecting the response of the biosensor. The effect of β-G loading from 5 to 40 mg mL^{-1} on the biosensor was investigated by keeping the GOD concentration at 5 mg mL^{-1} (Zhang et al., 2005). As shown in Fig. S3, the response current increased obviously as the β-G concentration increased, and then leveled off as the β-G concentration was more than 20 mg mL^{-1}. This could be attributed to enzyme reaction rate increasing with the increase of enzyme activity center, while the enzyme activity center could be entrapped by peptides as the enzyme concentration is too high, which could not facilitate the proceeding of the reaction. On the other hand, it was found that higher enzyme loading resulted in the increase of film thickness and the decrease of film stability, which decreased the reusability of biosensor. To make the biosensor stable and have a high response current, 20 mg mL^{-1} was optimized for the β-G concentration.

3.5. Effect of applied potential and solution pH on the biosensor response

The effect of applied potential on the biosensor response was investigated in the range from −0.3 to +0.2 V in 0.1 M PBS containing 50 μM β-glucan. As shown in Fig. 4(A), along with the increase of the applied potential the response current gradually increased, and then reached a maximum at 0.0 V. Further increasing the applied potential, the response current decreased. Therefore, an applied potential of 0.0 V was selected for further experiments.

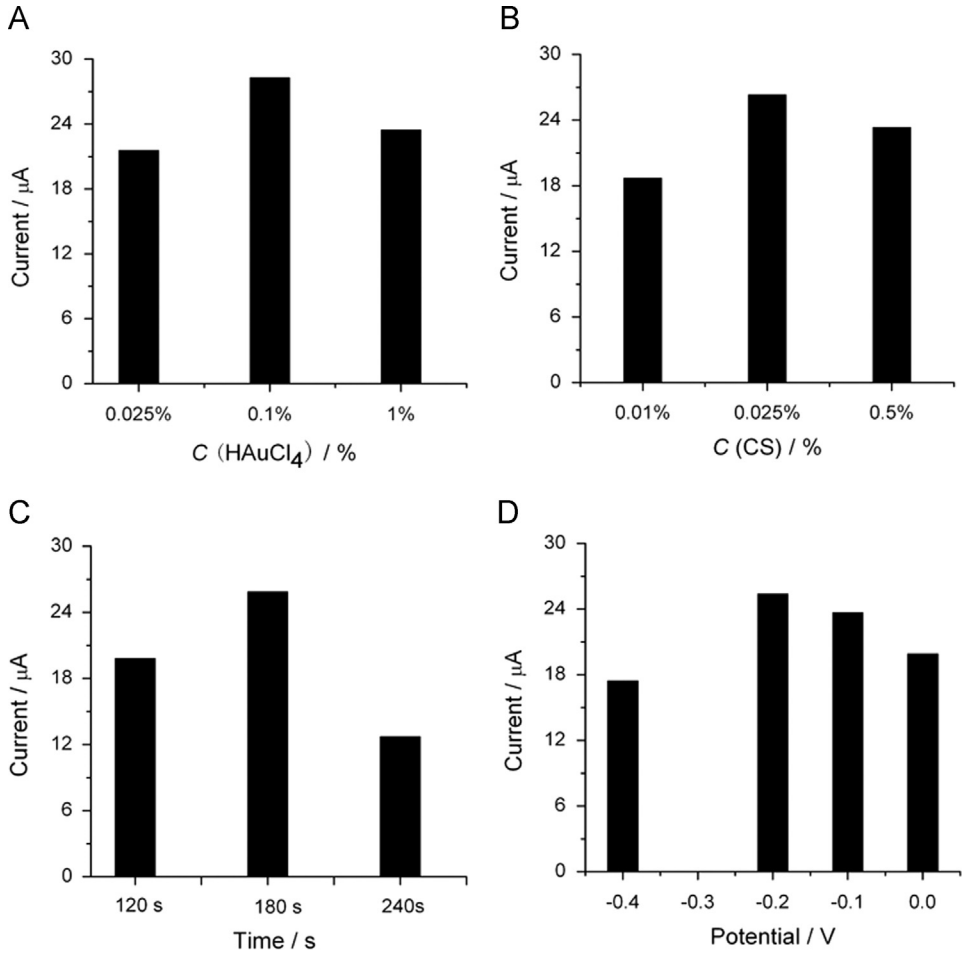

Fig. 3. Effect of the various deposition solution on the response current at AuNPs–CS/Au. The AuNPs–CS film deposited by chronoamperometry in (A) 0.025% CS with 0.025% $HAuCl_4$ (a), 0.1% $HAuCl_4$ (b), and 1% $HAuCl_4$ (c) for 240 s at −0.2 V, (B) 0.1% $HAuCl_4$ with 0.01% CS (a), 0.025% CS (b), and 0.05% CS (c) for 240 s at −0.2 V, (C) 0.1% $HAuCl_4$+0.025% CS for 120 s (a), 180 s (b), and 240 s (c) at −0.2 V, and (D) 0.1% $HAuCl_4$+0.025% CS for 180 s at −0.4 V (a), −0.2 V (b), −0.1 V(c), and 0.0 V (d).

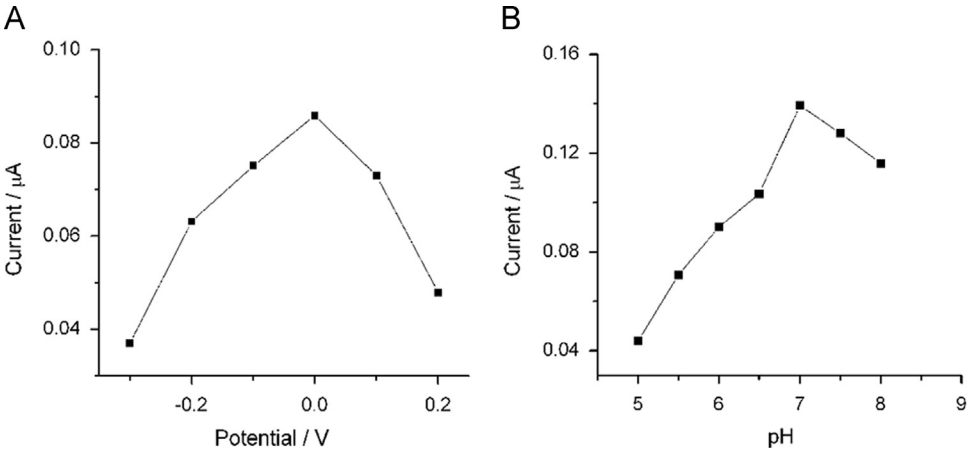

Fig. 4. Effect of applied potential (A) and pH (B) on the response current of the CS/β-G-GOD/AuNPs–CS/PB–CS/Au electrode in 0.1 M PBS containing 50 μM β-glucan.

The pH of solution can greatly affect the response of biosensor due to the bioactivity of enzyme and the stability of PB–CS depending on pH. Fig. 4(B) shows the response behavior of the biosensor in 0.1 M PBS containing 50 μM β-glucan in the pH range from 5.0 to 8.0. The response current of the biosensor increased sharply with the pH increasing from 5.0 to 7.0, and then decreased from 7.0 to 8.0. The maximum response current was observed at pH 7.0. Considering the sensitivity of the biosensor and practical biosensing application, the PBS of pH 7.0 was selected as the optimal supporting electrolyte.

3.6. Amperometric response of the biosensor towards β-glucan

In the presence of dissolved oxygen, glucose is generated during the oxidation of β-glucan catalyzed by β-G, followed by the generation of H_2O_2 during the enzymatic oxidation of glucose

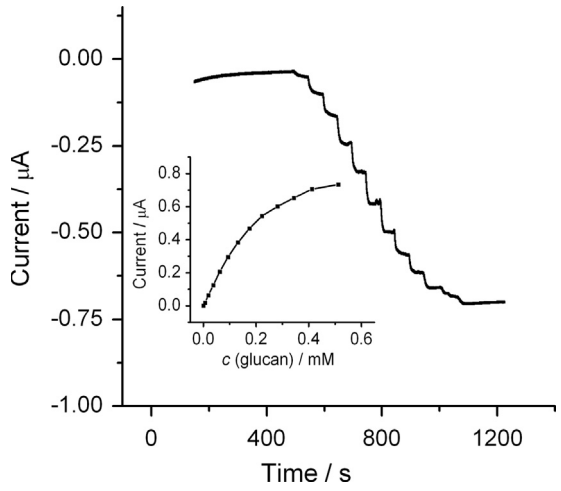

Fig. 5. Amperometric response obtained at the CS/β-G-GOD/AuNPs–CS/PB–CS/Au electrode in 0.1 M PBS (pH 7.0) on successive injection of 6.25, 12.5, 18.75, 25, 31.25, 37.5, 43.75, 50, 56.25, 62.5, 67.5 and 100 μM β-glucan. Inset, linear calibration curve between the response current and β-glucan concentration.

by GOD. The insoluble form of PB, $Fe_4^{III}[Fe^{II}(CN)_6]_3$, can be reduced to soluble Prussian White (PW), $K_4\{Fe_4^{II}[Fe^{II}(CN)_6]_3\}$ on the electrode, which has a catalytic activity for the reduction of H_2O_2 (Ji et al., 2010). Therefore, the response current of the catalytic reduction of H_2O_2 can be as the analytic signal for the determination of β-glucan. The reaction mechanisms of the biosensor could be described as follows (Bagal-Kestwal et al., 2009).

$$\beta\text{-D-glucan} + O_2 + H_2O + \beta\text{-G} \rightarrow \beta\text{-D-glucose} + H_2O \quad (1)$$

$$GOD(Ox) + \beta\text{-D-glucose} \rightarrow GOD(Red) + \beta\text{-D-gluconolactone} \quad (2)$$

$$GOD(Red) + O_2 \rightarrow GOD(Ox) + H_2O_2 \quad (3)$$

$$K_4\{Fe_4^{II}[\underset{PW}{Fe^{II}}(CN)_6]\} + 2H_2O_2 + 4H^+ \rightarrow \underset{PB}{Fe_4^{III}}[Fe^{III}(CN)_6]_3 + 4K^+ + 4H_2O \quad (4)$$

$$\underset{PB}{Fe_4^{III}}[Fe^{II}(CN)_6]_3 + 4K^+ + 4e^- \rightarrow K_4\{\underset{PW}{Fe_4^{II}}[Fe^{II}(CN)_6]_3\} \quad (5)$$

Fig. 5 displays a typical steady-state response of the biosensor on successive addition of β-glucan to 0.1 M PBS at the applied potential of 0.0 V. The biosensor exhibited a rapid and sensitive response to the changes of β-glucan concentration, reaching 95% of steady-state current within 10 s, which is two times as fast as that of β-glucan biosensor developed by Bagal-Kestwal et al. (2010). As shown in Fig. 5 (Inset), the biosensor presented a linear response to β-glucan concentration in the range from 6.25 to 93.75 μM (r=0.9991), with a detection limit of 1.56 μM. From the slope (3.14 nA μM^{-1} cm^{-2}) of the calibration curve, a sensitivity of 100 nA μM^{-1} cm^{-2} was obtained. With a further increase of β-glucan concentration, a plateau was observed, showing the characteristics of Michaelis–Menten kinetics (Salimi et al., 2007). The apparent Michaelis–Menten constant (K_m), which gives an indication of the enzyme-substrate kinetics for the biosensor, can be calculated from the Lineweaver–Burk equation (Shu and Wilson ,1976).

$$I_{ss}^{-1} = I_{max}^{-1} + K_m / I_{max} c^{-1}$$

where I_{ss} is the steady-state current after the addition of substrate, I_{max} is the maximum current measured under saturated substrate condition, and c is the bulk concentration of the substrate. The K_m value for the biosensor was estimated to be 1 mM, which is much smaller than that of β-glucan biosensor based on immobilization of tri-enzyme with AuNPs in agarose–cornflour–gelatin matrix (3.3 mM) (Bagal-Kestwal et al., 2010). The smaller K_m value means that the immobilized enzyme possesses higher catalytic activity, exhibiting an excellent affinity for β-glucan. It indicated that electrodeposited PB–CS/AuNPs–CS nanocomposite films are favorable candidates for the immobilization of enzymes because amine groups and cysteine residues in the enzymes could form chemical bonds with AuNPs (Luo et al., 2005), and enzymes immobilized on AuNPs can maintain their enzymatic for a considerable long time (Zhao et al., 1996). Moreover, CS is also an excellent immobilizing matrix and activity holder for enzymes (Wang et al., 2009). Therefore, the immobilization procedure affects on the enzymatic protein structure to a lesser extent, allowing to preserve a quite native-like one.

3.7. Anti-interference ability and stability of the biosensor

Fig. S4 presents the response current of the biosensor on the addition of β-glucan and several of electroactive interferents. It can be found that no obvious response current was observed on the injection of 30 μM UA, 2000 μM AP, and 20 μM AA, contrast to the large response to 50 μM β-glucan, showing that the biosensor had a good anti-interferent ability. It is attributed to two factors. One is the low applied potential due to the introduction of PB in nanocomposite film. Another is the chitosan cross-linking film on the outer layer of the electrode that forms a more compact network structure, which can restrain electroactive interferents from permeating into the film (Ji et al., 2010).

The stability of the biosensor under storage conditions (0.1 M PBS of pH 7.0 at 4 °C) was investigated by measuring the response current to 50 μM β-glucan in 0.1 M PBS. As shown in Fig. S5, the response current of the biosensor changed obviously in the first 3 days. However, one week later, the response current of the biosensor changed slightly, and remained ca. 82% of its original response current after 28 days. The good stability of the biosensor can be attributed to both the high affinity of AuNPs and the favorable bio-compatibility of chitosan to enzymes. The deposited PB–CS/AuNPs–CS nano-composite films and chitosan cross-linking film coated on the outer layer of the electrode can not only retain the bioactivity of the enzymes, but also effectively prevents the leakage of the enzymes (Ji et al., 2010).

4. β-glucan determination in samples

To investigate the potential application of the proposed biosensor, it was used for β-glucan assay in real samples analysis. β-glucan exists in oatmeal, fungi, yeast. Alcoholic drinks are manufactured by fermentation of fruits or grains with yeast, so three kinds of alcoholic drinks, oatmeal and hericium (fungi) were selected for the analysis of β-glucan. The oatmeal and hericium were crushed in a mortar with a pestle and dissolved in water, and their supernatants were used for determination, while the assay of alcoholic drinks without any pretreatment. A spectrophotometric method was used for the comparison of reliability and accuracy with the proposed biosensor. The results obtained from both methods are summarized in Table 1. The analysis of the correlation between the two methods gives the linear regression equation, y=1.264x −1876, and the correlation coefficient, R=0.9998, where y and x were the results obtained by the proposed biosensor and standard spectrophotometry, respectively. This indicated that the correlation between the two methods is very good. To further evaluate the accuracy of the proposed biosensor, three typical samples were selected for recovery test. The results are listed in Supplementary Table S1. The recoveries of the samples were observed in the range of 91.5–108.4%, which demonstrated good accuracy of the proposed biosensor for sample detection.

Table 1
Detection of β-glucan content in real samples.

Sample	Alcohol content (V/V) (%)	β-glucan concentration (mg L^{-1})[a]	
		Biosensor method	Standard method
Red wine	12	750 ± 4.34	785 ± 4.78
Beijing erguotou	56	905 ± 7.63	960 ± 9.22
Mianzhudaqu	42	670 ± 5.15	640 ± 6.46
Hericium	–	625 ± 3.11	600 ± 4.13
Oatmeal	–	1213 ± 12.8	1341 ± 14.3

[a] Average of three determinations ± SD, $n=3$

5. Conclusions

In this research, a β-glucan biosensor has been constructed based on efficient immobilization of bi-enzyme on the stable and controllable electrodeposited PB–CS and AuNPs–CS nanocomposite films. The AuNPs–CS nano-composite could efficiently facilitate electron transfer between the analyte and the surface of the electrode. Moreover, the PB–CS nanocomposite film lowered the applied potential, enhancing the selectivity of the biosensor. Both the nano-composite films containing chitosan displayed a 3-D superstructure with higher electrocatalytic activity, stability and uniform particle distribution. In addition, the chitosan coated on the surface of the biosensor not only offered a biocompatible environment for the enzymes, retaining the bioactivity of the enzymes, but also effectively prevented the leakage of the enzymes, increasing the stability of the biosensor. The resulting biosensor exhibited many advantages, such as, a rapid response, a wide linear range and a high affinity for β-glucan, and good storage stability.

Acknowledgments

This work was financially supported by the Natural Science Foundation of Hebei Province of China (No. B2010000844) and Research Foundation of Education Department of Hebei Province of China (No. ZH2012078).

Appendix A. Supplementary material

Supplementary data associated with this article can be found in the online version at http://dx.doi.org/10.1016/j.bios.2013.12.004.

References

Bai, X., Chen, G., Shiu, K.K., 2013. Electrochim. Acta 89, 454–460.
Bagal-Kestwal, D., Kestwal, R.M., Chiang, B.H., 2009. Biosens. Bioelectron. 24, 2566–2573.
Bagal-Kestwal, D., Kestwal, R.M., Hsieh, B.C., Chen, R.L.C., Cheng, T.J., Chiang, B.H., 2010. Biosen. Bioelectron. 26, 118–125.
Batra, B., Pundir, C.S., 2013. Biosens. Bioelectron. 47, 496–501.
Che, X., Yuan, R., Chai, Y., Li, J., Song, Z., Li, W., 2010. Electrochim. Acta 55, 5420–5427.
Chen, S., Yuan, R., Chai, Y., Xu, Y., Min, L., Li, N., 2008. Sens. Actuators B: Chem. 135, 236–244.
Clavaud, C., Beauvais, A., Barbin, L., Munier-Lehmann, H., Latge, J.P., 2012. Antimicrob. Agents Chemother. 56, 3428–3431.
Du, Y., Xu, J.J., Luo, X.L., Chen, H.Y., 2007. Bioelectrochemistry 70, 342–347.
Gamel, T.H., Badali, K., Tosh, S.M., 2013. J. Cereal Sci. 58, 104–109.
Gu, M., Zhang, J., Li, Y., Jiang, L., Zhu, J., 2009. Talanta 80, 246–249.
Hou, S., Ou, Z., Chen, Q., Wu, B., 2012. Biosens. Bioelectron. 33, 44–49.
Ji, X., Ren, J., Ni, R., Liu, X., 2010. Analyst 135, 2092–2098.
Karyakin, A.A., Karyakina, E.E., Gorton, L., 2000. Anal. Chem. 72, 1720–1723.
Koh, W.C.A., Chandra, P., Kim, D.M., Shim, Y.B., 2011. Anal. Chem. 83, 6177–6183.
Koichiro, Y., Yoshihito, N., Tadashi, M., Tomoyuki, Y., 2012. Igaku to Yakugaku 67, 895–902.
Liu, S., Xu, J., Chen, H., 2002. Electrochem. Commun. 4, 421–425.
Luo, X., Xu, J., Zhang, Q., Yang, G., Chen, H., 2005. Biosens. Bioelectron. 21, 190–196.
Mbhele, Z.H., Salemane, M.G., van Sittert, C.G.C.E., Nedeljkovic, J.M., Djokovic, V., Luyt, A.S., 2003. Chem. Mater.15, 5019–5024.
Ou, C., Yuan, R., Chai, Y., Tang, M., Chai, R., He, X., 2007. Anal. Chim. Acta 603, 205–213.
Park, B.W., Zheng, R., Ko, K.A., Cameron, B.D., Yoon, D.Y., Kim, D.S., 2012. Biosens. Bioelectron. 38, 295–301.
Pastuszka, D., Gambus, H., Ziobro, R., Buksa, K., Sabat, R., Augustyn, G., 2012. J. Microbiol. Biotechnol. Food Sci. 1, 972–979.
Regand, A., Chowdhury, Z., Wolever, T.M.S., Wood, P., 2011. Food Chem. 129, 297–304.
Salimi, A., Sharifi, E., Noorbakhsh, A., Soltanian, S., 2007. Biosens. Bioelectron. 22, 3146–3153.
Sanchez-Paniagua Lopez, M., Tamimi, F., Lopez-Cabarcos, E., Lopez-Ruiz, B., 2009. Biosens. Bioelectron. 24, 2574–2579.
Shu, F.R., Wilson, G.S., 1976. Anal. Chem. 48, 1679–1686.
Song, Y., Zhang, M., Wang, L., Wan, L., Xiao, X., Ye, S., Wang, J., 2011. Electrochim. Acta 56, 7267–7271.
Sorlier, P., Denuziere, A., Viton, C., Domard, A., 2001. Biomacromolecules 2, 765–772.
Wang, L., Ye, Y., Zhu, H., Song, Y., He, S., Xu, F., Hou, H., 2012. Nanotechnology 23 (455502), 10.
Wang, X., Gu, H., Yin, F., Tu, Y., 2009. Biosens. Bioelectron. 24, 1527–1530.
Wood, P.J., Weisz, J., Fedec, P., Burrows, V.D., 1989. Cereal Chem. 66, 97–103.
Yang, J., Myoung, N., Hong, H., 2012. Electrochim. Acta 81, 37–43.
Yang, W., Wang, J., Zhao, S., Sun, Y., Sun, C., 2006. Electrochem. Commun. 8, 665–672.
Yuan, C., Huang, X., Cheng, L., Bu, Y., Liu, G., Yi, F., Yang, Z., Song, F., 2009. Food Chem. 115, 581–584.
Zeng, J., Wei, W., Liu, X., Wang, Y., Luo, G., 2008. Microchimica. Acta 160, 261–267.
Zhang, Q., Zhang, L., Li, J., 2008. Electrochim. Acta 53, 3050–3055.
Zhang, S., Wang, N., Yu, H., Niu, Y., Sun, C., 2005. Bioelectrochemistry 67, 15–22.
Zhang, W., Xie, G., Li, S., Lu, L., Liu, B., 2012. Appl. Surf. Sci. 258, 8222–8227.
Zhao, J., O'Daly, J.P., Henkens, R.W., Stonehuerner, J., Crumbliss, A.L., 1996. Biosens. Bioelectron. 11, 493–502.
Zhao, S., Zhang, K., Bai, Y., Yang, W., Sun, C., 2006. Bioelectrochemistry 69, 158–163.
Zhong, X., Yuan, R., Chai, Y., 2012. Sens. Actuators B: Chem. 162, 334–340.